Investigation of liquid metallic wire heating dynamics

1997 J. Phys.: Condens. Matter 9 6175

(http://iopscience.iop.org/0953-8984/9/29/003)

J. Phys.: Condens. Matter **9** (1997) 6175–6184. Printed in the UK PII: S0953-8984(97)77664-1

Investigation of liquid metallic wire heating dynamics

N I Kuskova, S I Tkachenko† and S V Koval

Institute of Pulse Research and Engineering, National Academy of Sciences, pr. Oktyabrskii 43a, Nikolaev 327018, Ukraine

Received 6 September 1996

Abstract. The dynamics of a microsecond electric explosion of a tungsten wire in water is studied. A theoretical search for conditions of liquid wire radial uniformity is given. A new optical methods of temperature and radius measurements has been worked out. Mathematical modelling has been carried out to confirm the existence of radial uniformity and to compare the results with experimental and theoretical data. Conditions for the radial uniformity existence of liquid wire heating are presented; as tungsten uniform heating takes place at 10^{11} A m^{-2} $< j <$ 10^{12} A m^{-2}, one can use these regimes for investigation of the properties of liquid matter. The temperature dependence of liquid tungsten conductivity is given and compared with literature values. It is shown that vaporization begins with surface layers at chosen regimes of electric wire explosion.

1. Introduction

Acquiring knowledge on thermophysical properties of liquid metals is of considerable interest for most of the new energy technologies. Unfortunately direct measurements by static methods are impossible for most metals because of the extreme temperatures involved, especially for the refractory metals.

Therefore fast dynamic techniques have been used while measuring temperatures by optical methods. A more promising method is a method of wire self-heating by an electric current [1]. This method allows us to investigate a set of thermophysical properties of metals; the limitation of its applicability is caused by loss of the specimen uniformity. It is necessary to select the parameters of the specimen and the electric circuit in such a way that one can provide a stable process without losing the wire radial uniformity. We can see z-instabilities directly and we can avoid them by choosing parameters of the fine wire and the electric circuit. Therefore we must show that there is a radial uniformity of the exploding specimen in the range of parameters used.

At present uniform heating of solid specimens has been investigated well, but the uniformity of a liquid specimen has not been studied adequately. In this paper theoretical research on the radial uniformity of a liquid expanding wire is presented; theoretical results are compared with results of mathematical modelling and experimental data.

2. Theoretical model

The radial uniformity of the solid (nonexpanding) conductor caused by skin effects is well studied [2]. After wire melting there takes place its hydrodynamic expansion caused by

† Author responsible for correspondence.

0953-8984/97/296175+10$19.50

heating. Therefore there appears an additional item for the expression of the current density $j_z = \sigma(E_z + vB_\varphi)$ (where v is the expansion velocity of the heating wire, E_z is the electric field, B_φ is the magnetic induction and σ is the electrical conductivity). So, it is necessary to solve the diffusion equation of the magnetic field taking into account a wire expansion. The one-dimensional diffusion equation for cylindrical coordinates can be written

$$\frac{\partial B_\varphi}{\partial t} + \frac{\partial (vB_\varphi)}{\partial r} = \frac{1}{\mu\sigma}\frac{\partial}{\partial r}\left(\frac{1}{r}\frac{\partial (rB_\varphi)}{\partial r}\right) \tag{1}$$

with initial and boundary conditions

$$B_\varphi(r, t^0) = \frac{\mu I^0}{2\pi (a^0)^2} r \qquad B_\varphi(a, t) = \frac{\mu I}{2\pi a} \qquad B_\varphi(0, t) = 0 \tag{2}$$

where μ is the absolute magnetic permittivity, I is the heating current, a is the wire radius, and the superscript 0 refers to the moment of melting.

To find the conditions for radial uniformity of the current density we shall research the solution of a set of MHD equations describing uniform expansion of a circular liquid heating wire

$$\frac{\partial \rho}{\partial t} + \frac{\rho}{r}\frac{\partial (rv)}{\partial r} = 0 \tag{3}$$

$$\frac{\partial T}{\partial t} = \frac{I^2 R}{mc} \tag{4}$$

$$\rho\left(\frac{\partial v}{\partial t} + v\frac{\partial v}{\partial r}\right) = -\frac{\partial P}{\partial r} - \frac{0.5}{\mu r^2}\frac{\partial (r^2 B_\varphi^2)}{\partial r} \tag{5}$$

and the telegraph equation

$$L\frac{\mathrm{d}^2 I}{\mathrm{d}t^2} + \frac{\mathrm{d}(RI)}{\mathrm{d}t} + \frac{I}{C} = 0 \tag{6}$$

where m is the specimen mass; ρ is the mass density; T, P are the temperature and the pressure, respectively; c is the specific heat; L is the inductance; C is the capacitor capacitance; $R(t)$ is the resistance of the specimen involved. As there is no uniform analytic solution of the MHD equation set in cylindrical coordinates [3], we shall find a slightly nonuniform solution and this solution should be stable.

The initial and boundary conditions can be written at the moment of melting completion $t = t^0$

$$\begin{array}{llll} \rho(r, t^0) = \rho^0 & T(r, t) = T^0 & v(a, t) = \mathrm{d}a/\mathrm{d}t & v(0, t) = 0 \\ a(t^0) = a^0 & I(t^0) = I^0 & (\mathrm{d}I/\mathrm{d}t)^0 = \omega^0 I^0 & R(t^0) = R^0. \end{array} \tag{7}$$

We add the equation of state for the weak compressible medium which can be written as

$$\rho = \rho^0[1 - \alpha(T)(T - T^0)] \tag{8}$$

(where α is the thermal expansion coefficient), and also the temperature and density dependence of the conductivity which can be approximated by [4]

$$\sigma(\rho, T) = \frac{\sigma^0}{[1 + \beta(T - T^0)]}\left(\frac{\rho}{\rho^0}\right) \tag{9}$$

where β is the thermal coefficient of the conductivity for the liquid metal.

As a result of equation (3) the radial velocity of uniform wire expansion is $v(r, t) = (\mathrm{d}a/\mathrm{d}t)(r/a) = ur$ and the relation of the density to the wire radius is then given by $\rho/\rho^0 = (a^0/a)^2$.

If we assume that the following conditions are observed:

$$\tau_f \ll \sqrt{CL} \qquad \tau_f \ll (\beta A)^{-1} \qquad \tau_f \ll [\alpha(\delta-1)A]^{-1} \qquad \tau_f \ll (\omega)^{-1} \tag{10}$$

where τ_f is the lifetime of the uniformity; $A = (I^0)^2 R^0/(mc)$, then there are the approximate solutions of set (3)–(7)

$$\begin{aligned} I &\simeq I^0 \exp(\omega\tau) \qquad & R &\simeq R^0 + R_1\tau \\ a &\simeq a^0 \exp(u\tau) \qquad & T &\simeq T^0 + A\tau \end{aligned} \tag{11}$$

where $\tau = t - t^0$, $\omega = (\mathrm{d}I/\mathrm{d}t)^0/I^0$, $u = 0.5\alpha A$.

If $u < |\omega| \ll 4(\mu\sigma a^2)^{-1}$, then

$$B_\varphi \simeq \frac{\mu I}{2\pi a^2} r\left(1 + \frac{1}{8}\mu\sigma\omega r^2 + \frac{1}{192}(\mu\sigma)^2\omega(\omega+2u)r^4\right) \tag{12}$$

$$j \simeq \frac{I}{\pi a^2}\left(1 + \frac{1}{4}\mu\sigma\omega r^2 + \frac{1}{64}(\mu\sigma)^2\omega(\omega+2u)r^4\right). \tag{13}$$

Since the value ω may be either positive or negative, $j(a) > j(0)$ with $\omega > 0$, and $j(a) < j(0)$ with $\omega < 0$ can occur.

Substitution of (12) in (5) gives

$$P \simeq P(a,t) + \left[\frac{\mu I^2}{(2\pi a)^2}\left(1 + \frac{3(\mu\sigma\omega)^2}{16}(a^2+r^2)\right) + \frac{\rho}{2}\left\{a\frac{\mathrm{d}^2 a}{\mathrm{d}t^2} + \left(\frac{\mathrm{d}a}{\mathrm{d}t}\right)^2\right\}\right]\left(1 - \frac{r^2}{a^2}\right) \tag{14}$$

where $P(a,t)$ is the ambient pressure. One can estimate the nonuniformity depending on the magnetic pressure distribution. On estimating the critical value of the current density for liquid tungsten we can write $j_{cr} \sim 2\times 10^8/a^0$. If $a^0 \sim 0.2$ mm, then $j_{cr} \sim 10^{12}$ A m^{-2}, therefore we can conclude that the simple equation of state (8) for $j < 10^{12}$ A m^{-2} can be used.

3. Brief description of a specific system

The specimen was submerged in water in order to prevent shunt paths around the specimen.

In this work a fast bichromatic pyrometer is used to carry out temperature measurements. The radiation flow of the heated specimen is focused into the aperture plane, then it is collimated and after that it is directed to an optical dividing cube to form two optical channels. Each of the channels has its interference filter with different pass-bands.

In the present work six filters are used to expand a range of temperatures measured (wavelength centred on 415, 467, 530, 567, 606 and 656 nm with narrow-band $\Delta\lambda_i \sim$ 10 nm) and to cover the whole portion of the spectral sensibility of the detectors used. The radiation flows were registered by photomultipliers; at the same time heating current and specimen voltage drop were measured.

4. Details of measurements

4.1. Temperature

The thermal state of the specimen can be characterized by a conditional temperature, the so-called integral colour temperature (similar to [5])

$$\left(\int_{a_i^*}^{b_i^*} \varepsilon(\lambda,T) r(\lambda,T)\psi_{1i}(\lambda)\,\mathrm{d}\lambda\right)\left(\int_{a_j^*}^{b_j^*} \varepsilon(\lambda,T) r(\lambda,T)\psi_{2j}(\lambda)\,\mathrm{d}\lambda\right)^{-1} = \left(\int_{a_i^*}^{b_i^*} r(\lambda,T_{ic})\psi_{1i}(\lambda)\mathrm{d}\lambda\right)\left(\int_{a_j^*}^{b_j^*} r(\lambda,T_{ic})\psi_{2j}(\lambda)\,\mathrm{d}\lambda\right)^{-1} \tag{15}$$

where $\varepsilon(\lambda, T)$ is the emissivity, $r(\lambda, T)$ is the spectral density of a black body, T_{ic} is the integral colour temperature; ψ_{1i}, ψ_{2j} are the apparatus functions of the pyrometer channels; $(a_i^*, b_i^*) = (\lambda_i - 0.5\,\Delta\lambda_i,\ \lambda_i + 0.5\,\Delta\lambda_i)$ is the working range of the ith interference filter.

For the spectral density of a black body the Planck formula is used to determine the integral colour temperature from (15)

$$r(\lambda, T) = \frac{C_1}{\lambda^5}\left[\exp\left(\frac{C_2}{\lambda T}\right) - 1\right]^{-1} \tag{16}$$

where C_1 and C_2 are the first and second radiation constants, respectively.

In this paper the ratio of two pyrometer signals is used, therefore it is sufficient to have only the relative calibration of the channel sensibilities [6]

$$\frac{b_1(\lambda_i)}{b_2(\lambda_j)} = S_{ij}\left(\int_{a_i^*}^{b_i^*} r(\lambda, T_{ic})\psi_{1i}(\lambda)\,\mathrm{d}\lambda\right)\left(\int_{a_j^*}^{b_j^*} r(\lambda, T_{ic})\psi_{2j}(\lambda)\,\mathrm{d}\lambda\right)^{-1} \tag{17}$$

where b_i is the signal of the ith pyrometer channel; S_{ij} is the ratio of the relative calibration of pyrometer channels for each pair of filters, and it is achieved at calibrating by the filament tungsten lamp used as a light source.

So T_{ic} is the root of equation (17) with the right-hand side calculated by numerical integration. To determine a temperature with minimum error it is necessary to use a pyrometer signal from a nearest-neighbour pass-band of filters as the difference of emissivities for a nearest-neighbour wavelength will be vanishing with vanishing wavelength difference. If the temperature-dependent part of the emissivity $\varepsilon(T)$ is constant or is the same for different pass-bands one can use any pair of filters to determine the temperature.

4.2. Radius

The influence of the specimen expansion is excluded from the ratio b_1/b_2 but each of the pyrometer signals includes this information. We can write for the same channel at different moments

$$\frac{b(\lambda_i, t_2)}{b(\lambda_i, t_1)} \sim \frac{s(t_2)}{s(t_1)}\frac{f(T_2)}{f(T_1)} \tag{18}$$

where

$$f(T_{ic}) = \int_{a_i^*}^{b_i^*} r[\lambda, T_{ic}(t)]\psi_{1i}(\lambda)\,\mathrm{d}\lambda \tag{19}$$

$s(t) \sim a(t)d$ is the visible area of the emissive wire with an aperture; d is the aperture diameter ($a \ll d \ll l$; l is the length of the specimen).

If temperature dependences of emissivities differ much for different pass-bands and there exists a λ_j^* for which $\varepsilon(\lambda_j^*, T) \approx$ constant, then the information from pyrometer signals can be used for investigation of the dynamics of wire expansion. Such a wavelength λ_j^* is needed to diminish the errors of radius determination. The pyrometer signal in this wave can be used as a basic signal to find T_{ic}, which then is used to determine the wire radius. The more methodical the errors of radius measurements are, the more the emissivity $\varepsilon(\lambda_j^*, T)$ differs from a constant value.

Therefore the following ratio can be used to calculate the time dependent radius:

$$\frac{a(t)}{a(t^0)} = \frac{b(\lambda_i, t)}{b(\lambda_i, t^0)}\frac{f(T_{ic}^0)}{f(T_{ic})} \tag{20}$$

where $a(t^0)$ is the radius at the moment of melting completion, then t^0 is the moment of melting completion and T^0 is the melting temperature.

After calculating the integral colour temperature T_{ic} from (17), the ratio of pyrometer signals $b_1(\lambda_i, t)/b_2(\lambda_i, t^0)$ and the ratio of the functions $f(T_{ic}^0)/f(T_{ic})$ can be found, then the radius for each point of time can be determined from the product of these values and the radius at the melting moment.

In formula (17) the ratio $b_1(\lambda_i)/b_2(\lambda_j^*)$ is proportional to $\varepsilon(\lambda_i, T)/\varepsilon(\lambda_j^*)$; therefore if we use for radius determination $T_{ic}(t)$ (for metals with different dependences $\varepsilon(\lambda_i, T)$) then $T_{ic}(t)$ does not describe the real temperature $T(t)$, but is a function describing the change of temperature $T(t)$ and the change of emissivity $\varepsilon(\lambda_i, t)$ as well. Thus on determination of radius $a(t)$ using the temperature $T_{ic}(t)$ found from (17) upon λ_j^* is the same because the temperature dependence of emissivity $\varepsilon(\lambda_i, T)$ is taken into account.

5. Mathematical modelling

Mathematical modelling of a one-dimensional cylindric wire explosion was carried out for investigation of the radial uniformity. The set of MHD equations for the Lagrangian description and telegraph equation can be written

$$\frac{\mathrm{d}m}{\mathrm{d}t} = 0 \tag{21}$$

$$\rho\frac{\mathrm{d}v}{\mathrm{d}t} = -\frac{\partial P}{\partial r} - \frac{0.5}{\mu r^2}\frac{\partial(r^2 B_\varphi^2)}{\partial r} \tag{22}$$

$$\rho\frac{\mathrm{d}\varepsilon}{\mathrm{d}t} = -P\frac{1}{r}\frac{\partial(rv)}{\partial r} + \frac{1}{r}\frac{\partial}{\partial r}\left(\kappa r\frac{\partial T}{\partial r}\right) + \frac{j^2}{\sigma} + k(r)E_w \tag{23}$$

$$\frac{\mathrm{d}(\mu B_\varphi)}{\mathrm{d}t} = \frac{\partial}{\partial r}\left(\frac{1}{\sigma r}\frac{\partial(rB_\varphi)}{\partial r}\right) \tag{24}$$

$$\frac{\mathrm{d}^2(LI)}{\mathrm{d}t^2} + \frac{\mathrm{d}(RI)}{\mathrm{d}t} + \frac{I}{C} = 0 \tag{25}$$

where $\varepsilon(\rho, T)$ is the specific internal energy; E_w is the specific energy loss by superficial radiation; $k(r = a) = 1$, $k(r \neq a) = 0$, κ is the heat conductivity.

Specific conductivity can be calculated similarly (9); coefficients in this formula depend upon the phase diagram region for which this expression is written. Conductivity in the melting region can be determined from $\sigma = v\sigma_1(1 - v)\sigma_2$, where v is the volume concentration of phase 1; σ_1 and σ_2 are the conductivities of phases 1 and 2, accordingly. In the liquid–vapour coexistence region the conductivity can be defined as the conductivity of the effective medium [7], assuming that conductivity on the right branch of the P–V plane binodal is equal to zero. The heat conductivity can be calculated from $\kappa = k_{WF}T\sigma$ [4].

The evolution of the wire heating process at the initial stage can be simulated by equations (21), (23)–(25), assuming weak compressibility: $\rho = \rho_0\ [1 - \alpha(T)(T - T_0)]$, with the initial conditions defined at the moment of current switching on: $I(0) = 0$; $(\mathrm{d}I/\mathrm{d}t)_{t=0} = U_0/L$; $\rho(0, r) = \rho_0$; $T(0, r) = T_0$; $v(0, r) = 0$; $B_\varphi(0, r) = 0$; $j_z(0, r) = 0$. The flow parameters obtained at the moment of the melting completion can be taken as initial conditions for the set (21)–(25).

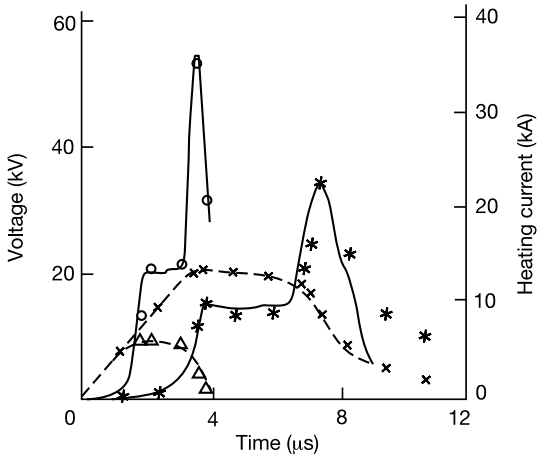

Figure 1. The time-dependent heating current and specimen voltage drop. ——, - - - -, numerical data for voltage and current respectively, ∗, ×, experimental data for voltage and current, respectively (regime 1); ○, △, experimental data for voltage and current, respectively (regime 2).

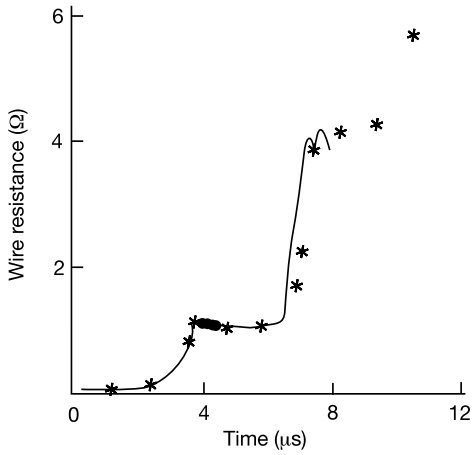

Figure 2. The time-dependent resistance of tungsten wire: ——, numerical data; ∗, experimental data; ●, data defined in accordance with (11).

The liquid and gas matter state can be described by Van der Waals–Maxwell equations

$$P = \frac{RT}{V-b} - \frac{a}{V^2} \qquad \varepsilon = \varepsilon^0 + c_v(T - T^0) + (\rho^0 - \rho) \tag{26}$$

$$\mu_f - \mu_g = \int_f^g \mathrm{d}\mu = \int_f^g V\,\mathrm{d}P = \int_f^g V\left(\frac{\partial P}{\partial V}\right)_T \mathrm{d}V = 0 \tag{27}$$

where $V = 1/\rho$ is the specific volume; μ_f and μ_g are the chemical potentials of liquid and gas accordingly; constants a and b can be calculated from ratios for the critical parameters, which were given in [8]; joining coefficients ε^0, T^0 and ρ^0 are determined at the melting point. Equation (26) is taken for specific internal energy with the specific heat equal to a constant. Equation (27) defines the medium behaviour in the liquid–vapour coexistence

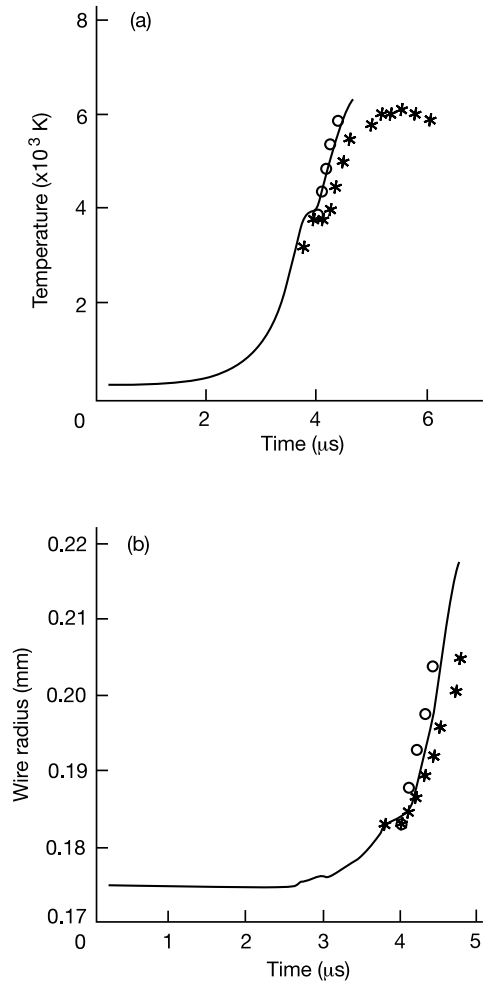

Figure 3. Time-dependent temperature (a) and radius (b) of tungsten wire: ——, numerical date; ∗, experimental data; ○, data defined in accordance with (11).

region. The equations (9), (26) and (27) give a qualitative description of the main properties of matter in the region of interest of the phase diagram (liquid metal and liquid–vapour coexistence region); a more correct description is rather difficult.

The boundary conditions at the symmetry axis can be defined as the conditions of cylindrical symmetry; the conditions at the outer boundary can be taken as the water parameters at normal conditions assuming the wire submerging into the infinite water medium described by the equation of state (26) and (27) with appropriate constants a and b.

6. Results

Optical investigation of temperature and radius for a cylindrical tungsten wire has been carried out for the following parameters: $a_{01} = 0.175$ mm, $l = 8.7$ cm, $L = 4.5$ μH, $C = 6$ μF, $U_0 = 20$ kV (regime 1) and also with a different initial wire radius $a_{02} = 0.1$ mm (regime 2).

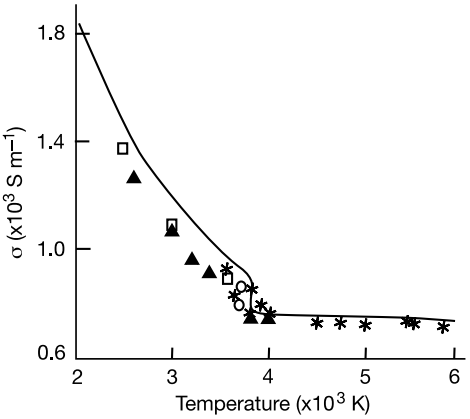

Figure 4. The temperature dependence of tungsten conductivity: ——, numerical data (formula (9) with $\beta = 2\times10^{-5}$ K^{-1} and $\delta = 0.67$ for liquid metal); *, experimental data; □, (9), ○, [10]; ▲, [11].

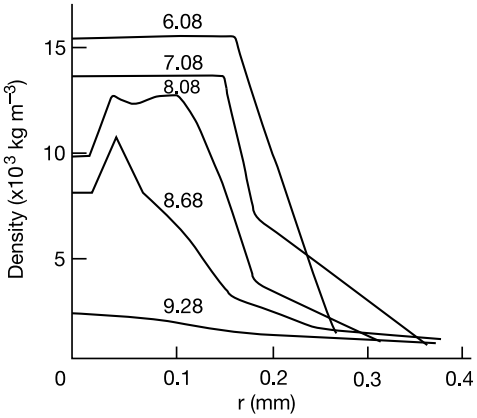

Figure 5. The propagation of boiling wave along the radius of a tungsten wire. Figures on the curves show the time in microseconds.

Mathematical modelling has been carried out for the same regimes. The coefficients $\delta = 0.67$ and $\beta = 2 \times 10^{-5}$ K^{-1} for liquid tungsten in formula (9) were found from the observed data of regime 1. Regime 2 was modelled with the same coefficients. The comparison of the numerical and experimental results for the heating current and the voltage in the two regimes can be seen in figure 1.

It is seen that the mathematical model describes well the mode of current and voltage change to the moment of the voltage peak, but after that a difference between the numerical and experimental data is noted.

The time-dependent resistance (figure 2) has three so-called ‘steps’. The first ‘step’ is caused by the resistance rise during heating at a solid phase (in this temperature range there exists a strong interdependence between conductivity and temperature) and during wire melting. The second ‘step’ corresponds to the time of the tungsten wire surface layer boiling and the third ‘step’ corresponds to boiling of inner layers. As the wire resistance increases up to vanishing current it is clear that breakdown does not take place in this process.

Analysing theoretical and numerical results one can conclude that regimes of tungsten electric explosion with 10^{11} A m^{-2} $< j <$ 10^{12} A m^{-2} are uniform, therefore it can be used for investigation of matter properties in the range from melting temperature to boiling temperature (under normal conditions). At $j < 10^{11}$ A m^{-2} and $j > 10^{12}$ A m^{-2} current redistributes along the radius because of the wire expansion and diffusion of the magnetic field.

As after preliminary calibration the melting temperature was found to differ by $\sim 5\%$ from the well known data, we carried out an additional calibration according to the melting temperature. After that the temperature of boiling was found to differ by $\sim 3\%$ from the well known data. This confirms the reliability of temperature measurements. The accurate estimation of methodical error in temperature and radius measurements is rather difficult.

Numerical, theoretical and experimental data of time dependence of temperature and radius are shown in figure 3(a) and (b) respectively. One can see that the thermal expansion coefficient was a little higher according to the above state equation. The time-dependent temperature (for the temperature range from melting to boiling upon the normal conditions) is in good agreement with experimental data. After that surface layers peel off on vaporizing and mix with surrounding water and this leads to cooling of these layers (such cooling was observed during experiments), therefore the experimental data for the processes taking place inside a wire cannot be obtained.

Numerical and experimental temperature-dependent conductivity is given in figure 4; for comparison the data obtained by other authors [9–11] are given too. The value of liquid tungsten conductivity changes from 0.755 to 0.690 MS m^{-1} (in the range of temperatures from melting to boiling); other authors give the following values: 0.685 [12]; 0.725 [13]; 0.730 [14]; 0.758 [15]; 0.787 [16]; 0.826 [17] MS m^{-1}.

One can see from the numerical results that on uniform heating of liquid metal matter vaporization begins with the wire surface; this is in agreement with experimental results [18]. The numerical data allow us to see the propagation of boiling wave from the surface to the centre of the wire. The radial distributions of density at different moments are shown in figure 5: one can see that phase transition occurs in a transition layer (with width $\delta_t \sim 50$–70 μm), which is a liquid–vapour coexistence region. The density diminishes about tenfold across the transition layer. The phase boundary moves to the wire centre with an average velocity equal to about 40 m s^{-1}. The velocity of the boiling wave can be estimated in an indirect way from experimental data. It can be seen from figures 1 and 3(a) that the boiling starts at the moment of the voltage rise $t \sim 5.2$ μs, and the completion of wire boiling probably corresponds to the current drop to vanishing value at the abrupt rising of the wire resistance (as the vapour is weakly conductive). Therefore the time for boiling wave propagation from surface to centre is $\tau_b \sim 6$ μS, and so the average velocity of this wave is $w \sim 30$ m s^{-1}. Thus numerical data are in agreement with experimental data.

7. Summary

As the experiments were carried out in a uniform heating regime, we can say that properties observed can be treated as average matter properties (in the range from melting to boiling temperatures). After the beginning of surface boiling the data for the surface processes cannot be taken as representative of the processes in the whole volume of the wire.

The conductivity of liquid tungsten changes slightly with rising temperature; this is in agreement with theory [19].

Numerical modelling shows that the boiling wave propagation from the surface to the centre of the wire has an average velocity of about 40 m s^{-1}; this result agrees well with indirect experimental data.

References

[1] Gathers G R 1986 *Rep. Prog. Phys.* **49** 341
[2] Landau L D and Lifshits E M 1982 *Theoretical Physics VIII* (Moscow: Nauka)
[3] Tkachenko S I 1995 *Math. Modelling* **7** 3
[4] Knoepfel H 1970 *Pulsed High Magnetic Fields* (North-Holland: Amsterdam)
[5] Krasnov K V, Osipov G I and Rostovtseva V V 1987 *Izmerit. Tekhn.* **3** 10
[6] Snopko V N 1992 *Izmerit. Tekhn.* **9** 37
[7] Kirkpatric S 1973 *Rev. Mod. Phys.* **45** 574
[8] Fortov V E, Dremin A N and Leont'ev A A 1975 *Teplofiz. Vys. Temp.* **13** 1072
[9] Cezarliyan A and McClure J L 1971 *J. Res. NBS* A **75** 283
[10] Lebedev S V and Savvatimski A I 1984 *Usp. Fiz. Nauk* **144** 215
[11] Desai P D, Chu T K, James H M and Ho C Y 1984 *J. Phys. Chem. Ref. Data* **13** 1069
[12] Hixson R S and Winkler M A 1990 *Int. J. Thermophys.* **11** 709
[13] Berthault A, Arles L and Matricon J 1986 *Int. J. Thermophys.* **7** 167
[14] Seydel U, Bauhof H, Fucke W and Wadle H 1979 *High Temp.–High Pressures* **11** 35
[15] Shaner J W, Gathers G R and Minichino C 1976 *High Temp.–High Pressures* **8** 425
[16] Savvatimski A I 1996 *Int. J. Thermophys.* **17** 495
[17] McClure J L and Cezairliyan A 1993 *Int. J. Thermophys.* **14** 449
[18] Koval S V and Kuskova N I 1995 *Pis. Zh. Tekh. Fiz.* **21** 36
[19] Mott N E and Davis E A 1979 *Electron Processes in Non-Crystalline Materials* (Oxford: Clarendon)